Use of 2D Sensitivity Encoding for Slow-Infusion Contrast-Enhanced Isotropic 3-T Whole-Heart Coronary MR Angiography

Article *in* American Journal of Roentgenology · August 2011

DOI: 10.2214/AJR.10.5724 · Source: PubMed

CITATIONS
3

READS
55

7 authors, including:

Bernhard Schnackenburg
Philips
181 PUBLICATIONS **5,571** CITATIONS
SEE PROFILE

Robert G Weiss
Johns Hopkins Medicine
232 PUBLICATIONS **7,728** CITATIONS
SEE PROFILE

Matthias Stuber
University of Lausanne
403 PUBLICATIONS **12,273** CITATIONS
SEE PROFILE

Cosima Jahnke
Heart Center Leipzig - University Hospital
165 PUBLICATIONS **2,558** CITATIONS
SEE PROFILE

Use of 2D Sensitivity Encoding for Slow-Infusion Contrast-Enhanced Isotropic 3-T Whole-Heart Coronary MR Angiography

Jing Yu[1,2]
Ingo Paetsch[3,4]
Bernhard Schnackenburg[5]
Eckart Fleck[3]
Robert G. Weiss[2,6]
Matthias Stuber[2,7]
Cosima Jahnke[3,4]

Keywords: coronary MR angiography, parallel imaging, signal-to-noise ratio

DOI:10.2214/AJR.10.5724

Received September 4, 2010; accepted after revision December 26, 2010.

Supported by NIH grants RO1 HL084186 and R01 HL084186-04S1 and the Donald W. Reynolds Foundation.

[1]Department of Biomedical Engineering, Johns Hopkins University, Baltimore, MD.

[2]Department of Radiology, Division of Magnetic Resonance Research, Johns Hopkins University, Baltimore, MD.

[3]Department of Internal Medicine/Cardiology, German Heart Institute Berlin, Berlin, Germany.

[4]Department of Cardiology, University Hospital RWTH Aachen, Pauwelsstrasse 30, 52074 Aachen, Germany. Address correspondence to C. Jahnke (cjahnke@alice.de).

[5]Philips Healthcare, Hamburg, Germany.

[6]Department of Medicine, Cardiology Division, Johns Hopkins University, Baltimore, MD.

[7]Department of Radiology, Centre Hospitalier Universitaire Vaudois and University of Lausanne, Center for Biomedical Imaging (CIBM), Lausanne, Switzerland.

AJR 2011; 197:374–382

0361–803X/11/1972–374

OBJECTIVE. The purpose of this study was to improve the blood-pool signal-to-noise ratio (SNR) and blood-myocardium contrast-to-noise ratio (CNR) of slow-infusion 3-T whole-heart coronary MR angiography (MRA).

SUBJECTS AND METHODS. In 2D sensitivity encoding (SENSE), the number of acquired k-space lines is reduced, allowing less radiofrequency excitation per cardiac cycle and a longer TR. The former can be exploited for signal enhancement with a higher radiofrequency excitation angle, and the latter leads to noise reduction due to lower data-sampling bandwidth. Both effects contribute to SNR gain in coronary MRA when spatial and temporal resolution and acquisition time remain identical. Numeric simulation was performed to select the optimal 2D SENSE pulse sequence parameters and predict the SNR gain. Eleven patients underwent conventional unenhanced and the proposed 2D SENSE contrast-enhanced coronary MRA acquisition. Blood-pool SNR, blood-myocardium CNR, visible vessel length, vessel sharpness, and number of side branches were evaluated.

RESULTS. Consistent with the numeric simulation, using 2D SENSE in contrast-enhanced coronary MRA resulted in significant improvement in aortic blood-pool SNR (unenhanced vs contrast-enhanced, 37.5 ± 14.7 vs 121.3 ± 44.0; $p < 0.05$) and CNR (14.4 ± 6.9 vs 101.5 ± 40.8; $p < 0.05$) in the patient sample. A longer length of left anterior descending coronary artery was visualized, but vessel sharpness, coronary artery coverage, and image quality score were not improved with the proposed approach.

CONCLUSION. In combination with contrast administration, 2D SENSE was found effective in improving SNR and CNR in 3-T whole-heart coronary MRA. Further investigation of cardiac motion compensation is necessary to exploit the SNR and CNR advantages and to achieve submillimeter spatial resolution.

Coronary MR angiography (MRA) has been found to be a valuable tool for the noninvasive detection of proximal coronary artery disease [1]. Whole-heart coronary MRA [2, 3] has the advantage of large volumetric coverage; both the left and right sides of the coronary arterial system can be imaged on one acquisition. In addition, no tedious and time-consuming planning acquisitions are needed, which substantially improves the ease of use of coronary MRA in general. Another major technical advance in coronary MRA is the clinical use of 3-T MRI systems. An increase in field strength from 1.5 T to 3 T supports higher blood-pool signal-to-noise ratio (SNR) and blood-myocardium contrast-to-noise ratio (CNR) while the acquisition sequences remain almost identical at both field strengths. Imaging at 3 T, however, is challenged by increased B0 field heterogeneity and constraints in specific absorption rate. Among the gradient-echo acquisition strategies, segmented k-space spoiled gradient-recalled echo (GRE) sequences have better tolerance to B0 field heterogeneity and a lower specific absorption rate than do steady-state free precession (SSFP) sequences. Therefore, although SSFP is widely used in 1.5-T coronary MRA, most 3-T coronary MRA studies have been conducted with GRE sequences [4]. However, major limitations of coronary MRA with spoiled GRE include the relatively low blood-pool SNR and blood-myocardium CNR compared with those of SSFP.

To improve contrast, various T1-shortening intravascular MRI contrast agents have been used for coronary MRA, and excellent image quality has been reported [5–8]. Meanwhile, image acquisition with slow infusion

of U.S. Food and Drug Administration–approved clinical extracellular contrast agents has emerged as a promising approach [9]. Nevertheless, and despite marked improvement in CNR after contrast administration, 3-T whole-heart coronary contrast-enhanced MRA (CE-MRA) has been found inferior to 1.5-T whole-heart SSFP unenhanced MRA [10]. Thus SNR continues to be limited in 3-T GRE sequences, constraining achievement of higher spatial and temporal resolution, which are critical to the diagnostic value of the technique.

Sensitivity encoding (SENSE) has been found effective for SNR enhancement [11, 12]. By reducing the number of k-space lines acquired in each heartbeat and thus prolonging TR, a reduced-signal-intensity readout bandwidth and more longitudinal magnetization relaxation contribute to a net SNR gain. The prolonged TR can be further exploited for additional SNR gain through the use of higher radiofrequency excitation angles. This effect is particularly magnified when blood T1 is much shortened. Therefore, the use of a SENSE approach in combination with an extracellular T1-lowering contrast agent seems particularly promising. Moreover, with the advent of 32-channel hardware, higher parallel imaging acceleration factors have become available and may particularly benefit 3D cardiovascular MRI. It is more SNR efficient to use a 2D SENSE acceleration factor of 2 × 2 than a 1D SENSE acceleration factor of 4 [13]. Previous reports [14, 15] on whole-heart coronary MRA have described the utility of 2D SENSE in abbreviating acquisition time without substantial loss of image quality. Yet the use of 2D SENSE for improving blood-pool SNR in whole-heart coronary CE-MRA has not been reported, to our knowledge.

We hypothesized that the combination of 2D SENSE and a high-relaxivity contrast agent could be a powerful method for achieving high SNR and CNR in 3-T whole-heart coronary MRA. A 2D SENSE accelerated spoiled GRE sequence was developed and optimized for high-resolution coronary CE-MRA with slow infusion of gadobenate dimeglumine (MultiHance, Bracco). The proposed method was first simulated and subsequently compared with conventional unenhanced MRA in a small patient cohort. Although the proposed technique was used with SENSE only, which is the parallel reconstruction method available on the clinical MRI system used in this study, the method theoretically can easily be combined with other parallel imaging techniques [16, 17], image based and k-space based alike, to achieve similar results.

Subjects and Methods

Theory

The SNR of a 3D segmented k-space spoiled GRE imaging technique as used for coronary MRA is related to voxel volume ($\Delta x\Delta y\Delta z$), steady-state transverse magnetization (M_{xy}), number of phase-encoding steps in both the y and z directions (N_y, N_z), signal sampling bandwidth (BW), and number of signals averaged (NSA). With a SENSE acceleration factor of R and associated geometry factor g, SNR is calculated with the following equation [11]:

$$\mathrm{SNR} \propto \frac{(\Delta x\Delta y\Delta z)\cdot M_{xy}\cdot\sqrt{N_yN_z}\cdot\sqrt{NSA}}{\sqrt{BW}\cdot g\cdot\sqrt{R}}$$

By replacing a 1D SENSE acceleration factor of 2 with a 2D SENSE acceleration of 2 × 2, the number of radiofrequency excitations per acquisition window can be halved without a change in acquisition time. With constant acquisition window duration, TR is doubled. If the time required for radiofrequency transmission and phase encoding does not change, the extra time made available per TR can be dedicated to signal sampling, and the sampling time is more than doubled. This means that bandwidth can be reduced more than twofold. As documented previously [11, 12], the increased efficiency of this radiofrequency receive–to–radiofrequency transmit duty cycle can be exploited for a substantial gain in SNR.

Meanwhile, in the case of CE-MRA, use of a prolonged TR and fewer radiofrequency excitations per acquisition interval increases longitudinal magnetization. This effect is particularly amplified if the blood T1 is shortened with contrast medium and helps not only to preserve the steady-state magnetization but also to minimize signal decay during the train of signal readouts in the acquisition window. As a result, reduced T1 and prolonged TR enable the use of greater radiofrequency excitation angles, which may lead to a substantial SNR advantage. The combined SNR advantage originating from the reduced sampling bandwidth and the increased radiofrequency excitation angle outweigh the SNR loss incurred by the use of an additional SENSE acceleration factor of 2. Therefore, a net SNR gain can be expected while acquisition time and spatial resolution remain unchanged.

Numeric Simulation

To investigate the theoretic blood SNR gain from 2D SENSE CE-MRA with optimized radiofrequency excitation angles relative to those of conventional unenhanced MRA, we performed numeric simulations of the Bloch equations using Matlab software (version 7, R14, MathWorks).

The baseline 3D unenhanced MRA sequence for comparison included a magnetization preparation pulse [18] (TE, 50), a spoiled GRE sequence, and a 1D SENSE acceleration factor of 2. The unenhanced blood T1 used for the simulation was 1550 ms [19], unenhanced T2 was 120 ms [20], and unenhanced T2* was 80 ms [20]. The pulse sequence parameters were closely matched to those used for coronary artery imaging, including acquisition window, 90 ms; TR/TE, 3.3/1.0; constant radiofrequency excitation angle (alpha), 20°; bandwidth, 540.1 Hz/pixel; g-factor, 1.06. The g-factor values used in the numeric simulation were measured on g-factor images reconstructed from coil sensitivity. The time-of-flight effect was not taken into account in the simulation. An artificial heart rate of 60 beats/min was used.

To study the effects of the contrast agent and prolongation of TR separately, we performed the sequence parameter optimization in two steps. The SNR of each step was computed and normalized to the baseline SNR. The first step was slow infusion of gadobenate dimeglumine. Use of gadobenate dimeglumine dramatically shortens blood T1 and T2. Thus the values used for numeric simulation were contrast-enhanced T1, 90 ms [21, 22]; contrast-enhanced T2, 35 ms [23]; and contrast-enhanced T2*, 30 ms. The contrast-generating preparation pulse was replaced by a nonselective inversion recovery preparation pulse with an inversion delay of 200 ms [9]. Except for radiofrequency excitation angle, all other sequence parameters including a 1D SENSE acceleration factor of 2 were identical to those of the unenhanced MRA baseline. This sequence is referred to as 1D SENSE CE-MRA, which is the contemporary protocol for slow-infusion coronary CE-MRA.

The second step was application of a 2D SENSE acceleration factor of 2 × 2 for CE-MRA. In an identical acquisition window duration of 90 ms, the number of radiofrequency excitations can be reduced from 27 to 14 for an increased TR and reduced signal-readout bandwidth. The parameters modified included TR/TE, 6.4/1.7; bandwidth, 153.0 Hz/pixel; and g-factor, 1.50.

To find the optimal radiofrequency excitation angle in each step, contrast-enhanced transverse magnetization of the first to the last radiofrequency excitation in the acquisition window after the inversion recovery preparation pulse was calculated with the Bloch equation. The simulation was repeated with incremental radiofrequency excitation angles of 20°, 25°, 30°, and 35°. The optimal radiofrequency excitation angle was then selected with the criterion that the signal intensity from the last radiofrequency excitation acquired in the ac-

quisition window is at least 60% of that of the first radiofrequency excitation. This 60% cutoff prevents drastic signal decay and pixel blurring as a result of the point-spread function. Simultaneously, the signal intensity from the first radiofrequency excitation should be maximized because it will be located in the center of the k-space in the concentric elliptic k-space ordering.

Patient Study

MRI protocol—All MRI studies were performed with a commercial 3-T whole-body MRI system (Achieva R2.6, Philips Healthcare). The MRI system was equipped with a 40 mT/m, 200 T/m/s gradient system and a 32-channel cardiac surface coil for signal reception. The study was approved by the local ethics committee, and written informed consent was obtained from all study participants.

Eleven patients (six women, five men; mean age, 55 ± 19 [SD] years) with suspected or known coronary artery disease who had not undergone coronary stent implantation or coronary artery bypass surgery underwent MRI in the supine position with the vector ECG electrodes connected to the anterior thorax. First, a multislice SSFP survey acquisition was performed in the axial, sagittal, and coronal planes to identify the heart and the lung-liver interface for navigator localization. This acquisition was followed by a SENSE reference acquisition with a spatial resolution of 11.0 × 15.1 × 15.0 mm (foot-head × right-left × anterior-posterior). A cine SSFP sequence (TR/TE, 3.2/1.7; alpha, 45°; temporal resolution, 38 ms) in the axial plane was performed in which the period of minimal right coronary artery (RCA) motion was visually identified.

After scout acquisition, baseline free-breathing navigator-gated (gating window, 6 mm) and corrected (foot-head correction with a correction factor of 0.45) [24] 3D unenhanced whole-heart coronary MRA with an adiabatic preparation pulse (TE, 50) was performed. The 3D k-space data were collected according to a concentric elliptic order in the two phase-encoding directions. During acquisition planning, the thickness of the 3D volume was adapted to heart size, but the in-plane FOV was always 210 × 260 mm (anteroposterior × right-left). Two saturation slabs in the sagittal direction were prescribed to suppress signal from the arms, and a third saturation slab in coronal orientation was positioned on the posterior aspect of the chest to suppress signal from the spinal cord. The acquired isotropic voxel size was 1.3 × 1.3 × 1.3 mm and interpolated to 0.65 × 0.65 × 0.65 mm during reconstruction. To accelerate image acquisition, a 1D SENSE acceleration factor of 2 was applied in the right-left direction. The duration of the acquisition window, ranging from 90 to 110 ms, was adjusted to the RCA rest period of individual patients. Other parameters were TR/TE, 3.3/1.1; bandwidth, 540.1 Hz/pixel; alpha, 20°.

A 0.2-mmol/kg dose of gadobenate dimeglumine was injected at 0.3 mL/s, and inversion recovery (inversion delay, 200 ms) CE-MRA acquisition was started 2 minutes after injection. The k-space filling order, spatial and temporal resolution, volumetric coverage, nominal acquisition time, and navigator pulse location remained unchanged relative to the baseline acquisition for the same patient. However, for CE-MRA, a 2D SENSE acceleration factor of 2 × 2 was used in the foot-head and right-left directions. Rather than being used to abbreviate acquisition time, 2D SENSE was exploited to maximize SNR by minimizing the signal readout bandwidth (TR/TE, 6.6/1.7, one-half the number of radiofrequency excitations per heartbeat compared with unenhanced MRA; bandwidth, 153.0 Hz/pixel) and by choosing an optimal alpha based on the numeric simulation. Selected parameters of unenhanced MRA and 2D SENSE CE-MRA are listed in Table 1.

To support SNR and CNR quantification on images acquired with SENSE, all whole-heart coronary acquisitions were automatically repeated with all radiofrequency excitations and gradients disabled (noise acquisition) [25]. The duration of the 3D noise acquisition was 30 seconds [12], no user interaction was required to perform the noise acquisition, and reconstruction of the noise data was automatically performed with the commercial reconstruction hardware of the system.

SNR and CNR computations—Regional SNR and CNR analyses were performed on the magnitude images. For blood-pool SNR quantification, a rectangular region of interest (ROI) was placed in the ascending aorta (ROI size, ≈ 250 pixels) at the level of the ostium of the left main coronary artery (LMCA). The signal intensity (SI_b) was measured as the mean intensity in the ROI on the anatomic image, and the noise was determined as the SD (SD_b) from the same ROI in the noise acquisition. The blood-pool SNR was then calculated as SI_b / SD_b. The SNR of blood in the coronary arteries also was calculated. For signal intensity measurements, small ROIs (size, ≈ 15 pixels) were placed in the LMCA and the proximal portion of the RCA on the anatomic image. To obtain adequate noise measurements, rectangular ROIs (size, > 250 pixels) were selected on the noise image and were localized at the same position as the small ROIs on the anatomic image. The SNR of the LMCA and proximal portion of the RCA were defined as the mean signal intensity in the coronary blood divided by the SD of noise intensity.

The myocardial signal intensity (SI_m), noise (SD_m), and thus SNR were measured from a rectangular ROI (size, ≈ 250 pixels) in the left ventricular myocardium in closest proximity to the LMCA. Finally, the blood-myocardium CNR was calculated as follows [26]: $(SI_b - SI_m) / [0.5 \times (SD_b + SD_m)]$.

Coronary MR angiographic evaluation—The 3D whole-heart MRA data sets were reformatted along the major axes of the RCA, left anterior descending coronary artery (LAD), and left circumflex artery (LCX) with the soap-bubble coronary MRA analysis software tool [27]. Objective measurements of visible vessel length were obtained on the reformatted images. Simultaneously, the average vessel sharpness along the entire visible length of the vessel was determined with the software. Coronary coverage was based on the numbers of visible coronary segments of major coronary arteries and major coronary branches according to the 15-segment classification of the American Heart Association [28].

Image quality with respect to the presence of artifacts was graded with a previously reported [1] 4-point scale, in which a grade of 1 indicated that > 50% of the coronary artery segments were not assessable; grade 2, that the coronary artery segments were visualized with moderate artifacts; grade 3, that mild artifacts were present on the images; and grade 4, that the coronary artery segments were visualized with minimum or no artifact. Coronary reformatting and visual scoring

TABLE 1: Selected Parameters for Unenhanced and 2D Sensitivity Encoding (SENSE) Contrast-Enhanced MR Angiographic Sequences

Parameter	Unenhanced	Contrast-Enhanced
SENSE acceleration factor	2 × 1	2 × 2
TR (ms)	3.3	6.4
Alpha	20°	To be determined
TE (ms)	1.1	1.7
Prepulse	T2 preparation	Inversion recovery
Voxel size (mm^3)		
Acquisition	1.3 × 1.3 × 1.3	1.3 × 1.3 × 1.3
Reconstruction	0.65 × 0.65 × 0.65	0.65 × 0.65 × 0.65

were performed by the same MRI scientist, who had more than 5 years of experience in coronary MRA. True blinding with regard to unenhanced and contrast-enhanced images was not practical because contrast-enhanced images had distinctly greater visual contrast. For patients who underwent catheterization for diagnostic purposes, coronary MRA images were compared with the radiographic angiograms.

Acquisition duration and navigator efficiency—In addition to the quantification of parameters related to image quality, the effective acquisition duration and the navigator efficiency were recorded.

Statistical analysis—All quantitative results were presented as mean ± 1 SD. A paired two-tailed Student *t* test was used to compare measurement results of SNR, CNR, vessel length, and vessel sharpness for 2D SENSE CE-MRA versus unenhanced MRA. The difference in coronary coverage and image quality score between 2D SENSE CE-MRA and unenhanced MRA was analyzed with the Wilcoxon signed rank test. A value of $p < 0.05$ was considered statistically significant.

Results

Numeric Simulation

According to the criteria defined, that is, maximizing initial signal intensity while limiting subsequent decay, the optimal angle for the 1D SENSE CE-MRA sequence was 20° and for the 2D SENSE CE-MRA sequence was 25°. Figure 1 shows the transverse magnetization of consecutive radiofrequency excitations in the acquisition used to select the optimal radiofrequency excitation angle for 2D SENSE CE-MRA. The optimal radiofrequency excitation angles, which are a function of the tissue properties (T1, T2, and T2*), sequence parameters (e.g., TR, acquisition window duration), and heart rate, vary at different magnetic field strengths but are expected to be identical on MRI systems from different manufacturers.

The SNR of unenhanced MRA was set at baseline. After infusion of the contrast agent and with a T1 of 90 ms, SNR was predicted to be improved approximately 179% in 1D SENSE CE-MRA. With optimized radiofrequency excitation angles and prolonged TR, use of 2D SENSE for CE-MRA was predicted to improve SNR approximately 217%. Thus 2D SENSE pulse sequence optimization led to SNR gain complementary to the SNR benefit associated with shortened blood T1.

Patient Study

All studies with or without gadobenate dimeglumine were successfully completed for all patients, providing adequate image quality for the subsequent analysis. Patient characteristics and left ventricular function at rest as assessed with MRI are summarized in Table 2.

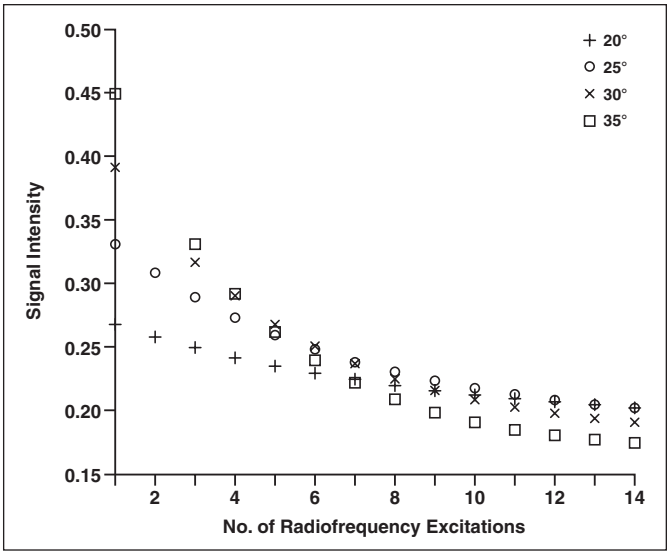

Fig. 1—Graph shows signal intensity of blood after contrast administration during acquisition window (90 ms) consisting of 14 constant radiofrequency excitations. Simulation has been made for readout trains with different radiofrequency excitation angles. With 25° radiofrequency excitation angle (*circles*), signal intensity for first readout is relatively high and decays smoothly during readout. Optimal radiofrequency excitation angle is approximately 25°.

Whole-heart 2D SENSE CE-MRA had a significantly higher blood-pool SNR and blood-myocardium CNR than did baseline unenhanced MRA (Table 3). The SNR of blood in the ascending aorta with the 2D SENSE CE-MRA method was threefold higher than that with baseline unenhanced MRA (37.5 ± 14.7 before vs 121.3 ± 44.0 after contrast enhancement, $p < 0.05$). The SNR of blood in the LMCA (28.1 ± 15.6 vs 85.0 ± 36.9, $p < 0.05$) and RCA (37.5 ± 14.1 vs 109.1 ± 41.9, $p < 0.05$) also was significantly improved with use of the 2D SENSE CE-MRA method. The percentage improvement in average SNR in the ascending aorta, LMCA, and proximal portion of the RCA was 223%, 203%, and 191%.

Table 3 also shows that the proposed technique did not equally benefit depiction of the three major vessels. The combined LMCA and LAD vessel length was significantly greater on 2D SENSE CE-MRA than unenhanced MRA images, but the vessel sharpness and the number of visible side branches

TABLE 2: Patient Demographics and Clinical Data

Characteristic	Value
Sex (no.)	
Men	5
Women	6
Age (y)	54.9 ± 19.3
Body mass index[a]	24.1 ± 2.5
Heart rate (beats/min)	63.2 ± 8.7
Cardiovascular risk factors (no.)	
Arterial hypertension	5 (46)
Diabetes mellitus	1 (9)
Hyperlipoproteinemia	4 (36)
Smoking	2 (18)
LV function	
LV ejection fraction (%)	58.1 ± 7.7
LV end-diastolic volume (mL)	138.7 ± 50.9
LV end-systolic volume (mL)	60.3 ± 31.9

Note—Values are mean ± SD or number. Values in parentheses are percentages. LV = left ventricular.
[a]Weight in kilograms divided by the square of height in meters.

TABLE 3: Signal-to-Noise Ratio, Contrast-to-Noise Ratio, Vessel Length, Vessel Sharpness, and Scan Duration for Unenhanced and Contrast-Enhanced Whole-Heart MR Angiography

Parameter	Unenhanced[a]	Contrast-Enhanced[b]
Signal-to-noise ratio		
Ascending aorta	37.5 ± 14.7	121.3 ± 44.0[c]
LMCA	28.1 ± 15.6	85.0 ± 36.9[c]
RCA	37.5 ± 14.1	109.0 ± 41.9[c]
Contrast-to-noise ratio (blood-myocardium)	14.4 ± 6.9	101.5 ± 40.8[c]
Vessel length (mm)		
LMCA + LAD (n = 10)[d]	79.7 ± 34.0	92.0 ± 33.9[c]
LCX (n = 10)[d]	33.6 ± 7.9	39.3 ± 10.6
RCA (n = 11)	117.8 ± 31.4	105.6 ± 36.8[c]
Vessel sharpness (%)		
LMCA + LAD (n = 10)[d]	49.1 ± 7.4	46.5 ± 7.2
LCX (n = 10)[d]	51.1 ± 8.7	42.7 ± 7.5[c]
RCA (n = 11)	51.5 ± 7.4	52.0 ± 11.1
Scan duration (min)	9.7 ± 3.6	12.3 ± 7.7
Navigator efficiency (%)	52.3 ± 13.0	47.9 ± 10.7

Note—LMCA = left main coronary artery, RCA = right coronary artery, LAD = left anterior descending coronary artery, LCX, left circumflex artery.
[a]T2 preparation pulse, 1D sensitivity encoding (SENSE).
[b]Gadobenate dimeglumine, 2D SENSE.
[c]$p < 0.05$ versus T2 preparation pulse values (paired two-sided Student t test).
[d]Not visualized in one patient.

did not change significantly. A trend for longer visible vessel segments was also measured for the LCX in the comparison of 2D SENSE CE-MRA and unenhanced MRA, but it did not reach statistical significance. However, the vessel sharpness of the LCX obtained with 2D SENSE CE-MRA was significantly lower than that with unenhanced MRA. In contrast to the left coronary artery system, the visible RCA length did not benefit from 2D SENSE CE-MRA, and RCA vessel sharpness and visibility of side branches remained largely unaffected compared with the findings at unenhanced MRA. Although the average duration of unenhanced MRA acquisition was less than that of 2D SENSE CE-MRA, this finding was only a trend and did not reach statistical significance (Table 3).

Table 4 shows that no statistical difference was found in the number of visible major coronary arteries (80/99 before vs 78/99 after contrast enhancement) and main side branches (19/66 vs 17/66) between 2D SENSE CE-MRA and unenhanced MRA. The mean scores of image quality of the two techniques also were close (2.8 ± 0.8 before vs 2.7 ± 0.9 after contrast enhancement).

Figure 2 shows a soap-bubble reformatted LAD and a first diagonal branch in the same patient on both unenhanced MRA (Fig. 2A) and 2D SENSE CE-MRA (Fig. 2B) images. Both images show the LMCA and a long segment of the LAD. However, the more distal LAD and diagonal branch are more evident on the contrast-enhanced image, on which signal suppression of the myocardium improved blood-myocardium contrast.

Another important aspect of visualization of the left coronary artery system is highlighted in Figure 3, which shows reformatted images of an LCX and the intermediate branch without (Fig. 3A) and with (Fig. 3B) a contrast agent. The tortuous course of the intermediate branch was depicted very well on both images, but the 2D SENSE CE-MRA images had better vessel conspicuity and longer visible distal segments. However, the signal intensity of the great cardiac vein appeared to increase after contrast administration, and the vein ran partly in parallel to the LCX. As a result and consistent with the reduced quantitative vessel sharpness of the LCX after contrast administration, the LCX was no longer distinct from the great cardiac vein, and therefore delineation was compromised on the 2D SENSE CE-MRA images.

Representative images of the RCA are displayed in Figure 4. Compared with the corresponding unenhanced MRA image (Fig. 4A), the 2D SENSE CE-MRA image (Fig. 4B) shows improved delineation of the RCA, and vessels of very similar length are visualized. Although other structures, such as the chest wall, are visible on the unenhanced image, the signal intensity in these regions is almost entirely suppressed after contrast administration, leading to more exclusive depiction of the blood-pool. All 2D SENSE CE-MRA images in Figures 2–4 show substantially enhanced blood-pool SNR and well-suppressed surrounding tissues, such as myocardium, skeletal muscle, and fat.

Two of the 11 patients in this study underwent radiographic coronary angiography for diagnostic purposes, and one was found to have significant stenosis. The images are shown in Figure 5. The locations of the stenoses identified on 2D SENSE CE-MRA images agreed well with those on the conventional angiograms. In comparison, the right marginal branch of the RCA, which was identified with 2D SENSE CE-MRA, was not depicted on the unenhanced MRA image.

Discussion

In this study of patients undergoing whole-heart coronary MRA with slow infusion of an extracellular contrast agent (gadobenate dimeglumine), we found that use of the contrast agent in concert with 2D SENSE led to substantial improvement in SNR and CNR compared with the results with the unenhanced technique. Therefore, this study showed that the combination of 2D SENSE

TABLE 4: Coronary Coverage and Image Quality Score for Unenhanced and Contrast-Enhanced Whole-Heart MR Angiography

Variable	Unenhanced[a]	Contrast-Enhanced[b]
No. of major coronary arteries	80/99 (81)	78/99 (79)
No. of main coronary branches	19/66 (29)	17/66 (26)
Score of image quality	2.8 ± 0.8	2.7 ± 0.9

Note—Values in parentheses are percentages.
[a]T2 preparation pulse, 1D sensitivity encoding (SENSE).
[b]Gadobenate dimeglumine, 2D SENSE.

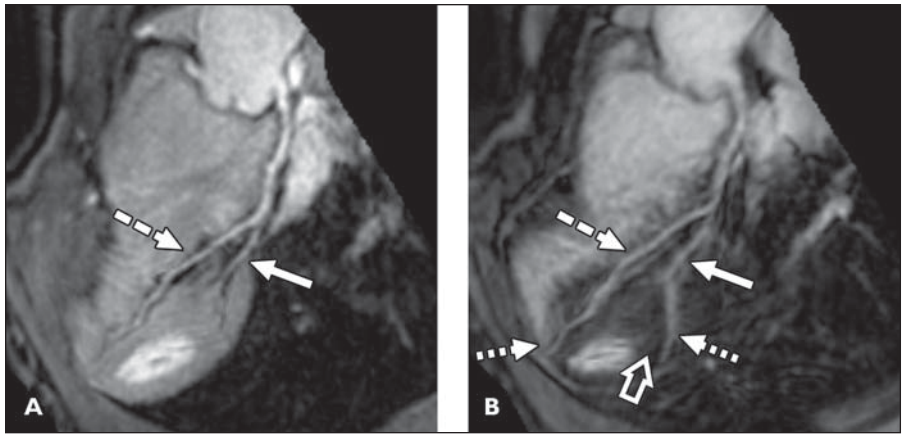

Fig. 2—21-year-old woman with atypical chest pain.
A and **B,** Representative reformatted unenhanced (**A**) and 2D sensitivity-encoded contrast-enhanced (**B**) MR angiograms show left anterior descending coronary artery (LAD) (*dashed arrow*) and first diagonal branch (*solid arrow*). Both longer LAD and distal first diagonal branch (*dotted arrows,* **B**) are visible in **B** but not in **A**. **B** shows good suppression of myocardial signal (*open arrow*).

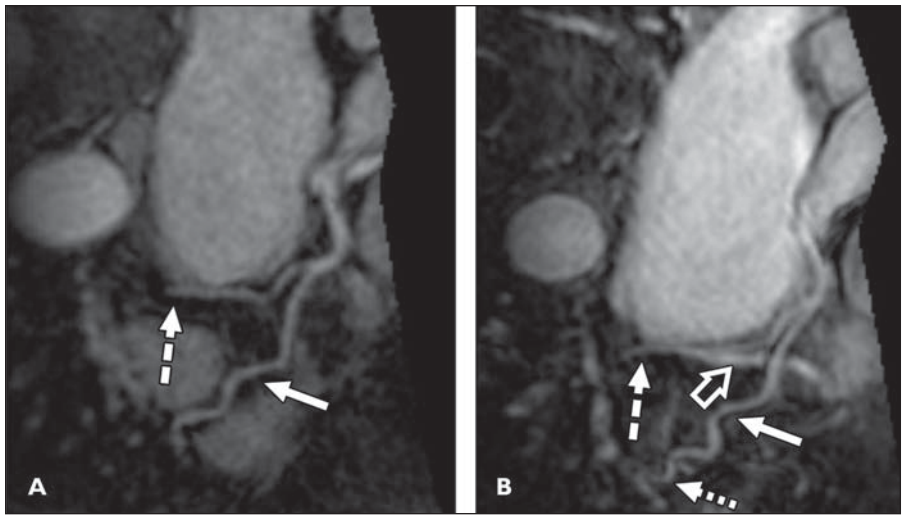

Fig. 3—68-year-old woman with suspected coronary artery disease.
A and **B,** Unenhanced (**A**) and sensitivity-encoded contrast-enhanced (**B**) MR angiograms show left circumflex artery (LCX) (*dashed arrow*) and intermediate branch (*solid arrow*). Distal LCX (*dashed arrow*) and ramus intermedius (*dotted arrow,* **B**) are better depicted in **B,** but mid LCX is overlapped by great cardiac vein (*open arrow,* **B**).

and a high-relaxivity contrast agent can be used to achieve high SNR and CNR in 3-T whole-heart coronary MRA. Overall, threefold improvement in blood-pool SNR was measured in a patient population with suspected or known coronary artery disease.

The slight difference in percentage SNR measurements in the ascending aorta, LMCA, and RCA may be attributable to the distance between the structure and the coil. In the LMCA and RCA, where the ROIs barely avoided pixels at the vessel boundary, vessel signal intensity might have been compromised by the partial volume effect. In general, 3D imaging affords an SNR advantage compared with multislice 2D approaches with identical spatial resolution. With the administration of T1-shortening contrast agents, approximately twofold improvement in SNR has been reported [9]. By exploiting the 2D SENSE technique and combining it with both a prolonged TR and a higher radiofrequency excitation angle, we obtained an extra SNR benefit that surpassed the twofold improvement attributable to shortened blood T1 after contrast administration. The additional SNR benefit can be attributed to noise reduction secondary to the reduced bandwidth and to signal enhancement due to a higher radiofrequency excitation angle. The quantitative SNR improvement agreed well with the numeric simulation results. The numeric simulation also showed the SNR benefits associated with T1 shortening caused by the contrast agent in conjunction with the proposed 2D SENSE pulse sequence.

In 2D SENSE CE-MRA, long, contiguous contrast-enhanced segments of the left and right coronary arterial system were consistently imaged during free breathing in patients with suspected or known coronary artery disease. The visible length of the combined LMCA and LAD was significantly greater on 2D SENSE CE-MRA than on unenhanced MRA images (Table 3). As shown in Figure 2, the middle and distal segments of the LAD along with its side branches can be better delineated because of improved myocardial signal suppression on the contrast-enhanced images. Similar findings of improved depiction of distal coronary arteries have been reported in previous studies of coronary CE-MRA [5, 7, 10].

Although more side branches were depicted, visualization of the LCX after contrast administration remains challenging because of simultaneous enhancement of the great cardiac vein, which often runs parallel to the middle and distal LCX. Thus in addition to improved SNR and CNR, further increased spatial resolution and venous blood-signal suppression remain important requirements for adequate visualization of the LCX after contrast enhancement. For the RCA, no statistically significant improvement was found after contrast enhancement. This finding may be explained by the fact that the RCA is embedded in more pericardial fat than is the LCA; therefore, attenuation of the fat signal rather than myocardial signal is the major determinant of contrast. In addition, the RCA usually is close to the anterior chest wall and to the anterior radiofrequency coils used for signal reception. This configuration may explain why high-quality depiction of the RCA can be achieved at coronary MRA without contrast agents.

Despite enhanced SNR and CNR, vessel sharpness, which serves as an objective measure of vessel conspicuity, was not improved. These findings were not entirely consistent with those of other studies [5, 8, 29], in which use of contrast agents significantly improved vessel sharpness in comparison with baseline unenhanced imaging. However, this result may be attributable to the use

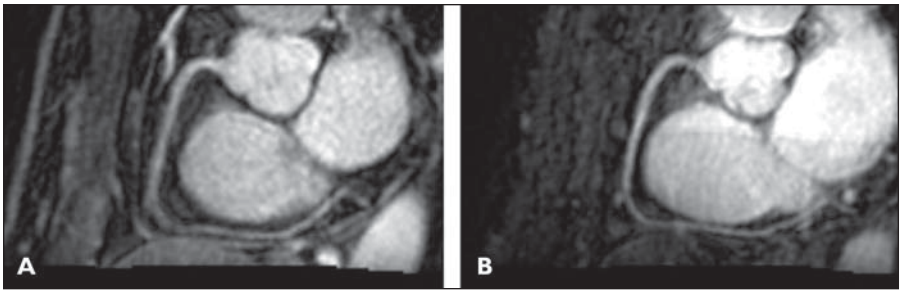

Fig. 4—68-year-old woman with suspected coronary artery disease (same patient as in Figure 3).
A and **B,** Unenhanced (**A**) and 2D SENSE contrast-enhanced (**B**) MR angiograms show right coronary artery (RCA).

of intravascular contrast agents and different injection schemes in the various studies. Intravascular contrast agents such as B-22956 [8, 29] and gadofosveset trisodium (Vasovist, Bayer Schering Pharma) [5], have a considerably longer plasma half-life (224 ± 30 minutes and 2–3 hours) than does gadobenate dimeglumine (20 minutes) [30]. Therefore, such intravascular contrast agents are particularly well suited for coronary MRA with prolonged acquisition times. In general, each whole-heart coronary MRA acquisition can be completed within 15 minutes after contrast injection, including the 2-minute waiting time during the initial infusion. With gadobenate dimeglumine, although blood T1 increases only slightly during the image acquisition period [22], the extracellular distribution and diffusion of unbound gadobenate dimeglumine molecules into the vessel wall can affect vessel depiction. In a study of a series of breath-hold coronary MRA images obtained at different delays after a single injection of gadofosveset trisodium, increased vessel edge blurring was found within 30 minutes after injection [6]. Thus in coronary CE-MRA, the kinetics of the contrast agent may not only influence the point-spread function related to the signal intensity variation in the k-space but also influence uptake kinetics into the vessel wall [31], and the effects on MR angiograms remain to be investigated. In this regard, abbreviated acquisition times may help to mitigate the unwanted effects.

Although 2D SENSE CE-MRA did not have significantly better image quality than unenhanced MRA (Table 4), the SNR gain associated with the proposed technique holds great promise for high spatial resolution, which has been emphasized for better coronary artery delineation and diagnostic value of coronary MRA [32]. The current study was conducted with an isotropic voxel size of 1.3 mm. Because of the isotropy of the voxels, any arbitrary viewing plane in the 3D data set can be freely selected with identical image quality. The SNR gain obtained in this study may have important implications for submillimeter isotropic resolution. However, it should be noted that the effective resolution not only is limited by SNR and point-spread function but also is determined by cardiac and respiratory motion. Studies have shown that free-breathing navigator technique with motion compensation suffers from nonnegligible residual motion of the coronary arteries [33]. Therefore, before implementation of whole-heart coronary MRA with further improvement in isotropic spatial resolution, a major focus on motion artifact suppression is mandatory. These efforts should be directed at reducing the residual coronary motion uncertainty to dimensions markedly smaller than the acquired voxel size.

To the best of our knowledge, this report is the first describing application of 2D SENSE to contrast-enhanced whole-heart coronary artery imaging. In this context, two specific aspects of 2D SENSE merit discussion. First, use of 2D SENSE with a moderate acceleration factor of 2 × 2 enabled by advanced 32-channel radiofrequency phased-array architecture effectively avoids drastic deterioration of the g-factor. With use of adequately localized spatial saturation slabs, no unfolding errors were identified at the level of the heart. Particularly on contrast-enhanced images on which much of the signal intensity outside the heart is reduced because of the nonselective inversion recovery prepulse, deterioration of the g-factor may be even less of a concern. Second, SENSE acceleration was simultaneously obtained in the right-left and foot-head directions, which are the optimal acceleration directions for the current coil geometry. Previous 2D SENSE accelerated whole-heart MRA studies were performed with foot-head and anteroposterior as the two phase-encoding directions to shorten acquisition time because the FOV of the human chest is typically smaller in the anteroposterior than in the right-left direction [14]. In our study, we chose foot-head and right-left to minimize the g-factor and kept the acquisition time at approximately 10 minutes using pulse sequence parameter optimization.

In this study we used a delay time of 2 minutes between contrast injection and data

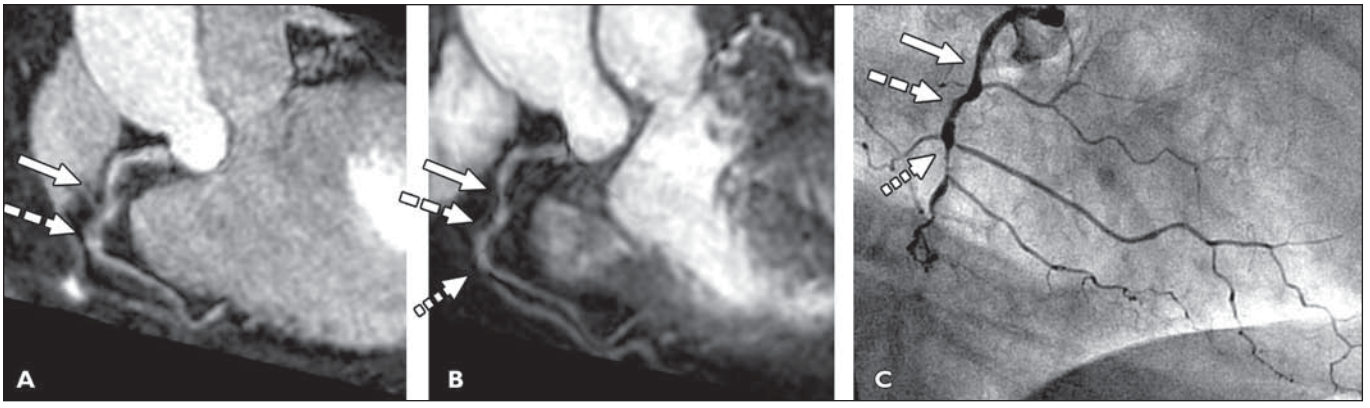

Fig. 5—76-year-old man with coronary artery disease.
A–C, Multiplanar reformatted unenhanced (**A**) and 2D sensitivity-encoded contrast-enhanced (**B**) MR angiograms and corresponding radiographic angiogram (**C**) show three sites of stenosis in right coronary artery (RCA) (*arrows*). Locations of luminal narrowing in proximal and mid RCA in **B** agree well with those in **C.**

acquisition. With a 0.2-mmol/kg contrast dose and 0.3 mL/s injection rate, infusion of the contrast agent was completed within 90–120 seconds. As previously reported [34], if concentric elliptical k-space data acquisition starts early during slow infusion, images of the center of the k-space region can be acquired before the lowest blood T1 is attained. This method has been reported to result in ghosting and blurring in coronary MRA. We avoided such artifacts by using a delay time of 2 minutes. In addition, peak enhancement often occurs soon after completion of injection. A delay of 2 minutes was therefore expected to be a good approximation of the time of peak contrast enhancement in general. An innovative self-triggered method has been proposed [35] whereby acquisition is started automatically when the peak blood signal enhancement is detected by the MRI unit. In this way, the delay time is tailored to the individual patient to account for variations in physiologic conditions. This sophisticated approach, however, was not available for the current study. More detailed investigations of 2D SENSE CE-MRA with optimal and individually adapted delay times may be warranted.

Several limitations of this study should be acknowledged. First, for practical reasons, the presentation of unenhanced MRA and 2D SENSE CE-MRA images was not randomized. Unenhanced MRA was always performed before 2D SENSE CE-MRA to avoid the lingering effect of the contrast agent. Second, a single injection of double-dose gadobenate dimeglumine (0.2 mmol/kg) was administrated in the study. Although use of a high dose might have been beneficial, the side effects, particularly in patients with impaired renal function, have to be considered. In addition, because of the use of double-dose gadobenate dimeglumine, one contrast-enhanced whole-heart MRA acquisition, which already occupied the peak enhancement duration, could be performed for each subject. The lack of intrasubject comparison between 2D SENSE CE-MRA and CE-MRA without 2D SENSE, and thus direct assessment of the effect of 3D acquisition alone on SNR, was another limitation. Finally, the sample size was small. Prospective clinical studies with a larger sample of patients with coronary artery disease that includes comparison with the angiographic standard of reference would be desirable for corroboration of the clinical usefulness of the proposed technique.

Conclusion

The combination of 2D SENSE and contrast administration substantially improves blood-pool SNR and blood-myocardium CNR at 3 T and supports isotropic whole-heart coronary MRA at high spatial resolution. The proposed technique enables longer visualization of the LAD, and the vessel sharpness, coronary artery coverage, and image quality score are similar to those of the unenhanced MRA baseline. Further improved motion compensation techniques aimed at substantial reduction of residual coronary motion are needed. This step will be critical to taking full advantage of the SNR and CNR benefits of the current 2D SENSE CE-MRA approach.

Acknowledgments

The authors thank Michael Schär, Philips Healthcare, for helpful discussions and Sebastian Kelle, German Heart Institute Berlin, for manuscript editing.

References

1. Kim WY, Danias PG, Stuber M, et al. Coronary magnetic resonance angiography for the detection of coronary stenoses. *N Engl J Med* 2001; 345: 1863–1869
2. Weber OM, Martin AJ, Higgins CB. Whole-heart steady-state free precession coronary artery magnetic resonance angiography. *Magn Reson Med* 2003; 50:1223–1228
3. Jahnke C, Paetsch I, Nehrke K, et al. Rapid and complete coronary arterial tree visualization with magnetic resonance imaging: feasibility and diagnostic performance. *Eur Heart J* 2005; 26:2313–2319
4. Stuber M, Botnar RM, Fischer SE, et al. Preliminary report on in vivo coronary MRA at 3 Tesla in humans. *Magn Reson Med* 2002; 48:425–429
5. Kelle S, Thouet T, Tangcharoen T, et al. Whole-heart coronary magnetic resonance angiography with MS-325 (Gadofosveset). *Med Sci Monit* 2007; 13:CR469–CR474
6. Nassenstein K, Waltering KU, Kelle S, et al. Magnetic resonance coronary angiography with Vasovist: in-vivo T1 estimation to improve image quality of navigator and breath-hold techniques. *Eur Radiol* 2008; 18:103–109
7. Prompona M, Cyran C, Nikolaou K, Bauner K, Reiser M, Huber A. Contrast-enhanced whole-heart MR coronary angiography at 3.0 T using the intravascular contrast agent gadofosveset. *Invest Radiol* 2009; 44:369–374
8. Paetsch I, Huber ME, Bornstedt A, et al. Improved three-dimensional free-breathing coronary magnetic resonance angiography using gadocoletic acid (B-22956) for intravascular contrast enhancement. *J Magn Reson Imaging* 2004; 20:288–293
9. Bi X, Carr JC, Li D. Whole-heart coronary magnetic resonance angiography at 3 Tesla in 5 minutes with slow infusion of Gd-BOPTA, a high-relaxivity clinical contrast agent. *Magn Reson Med* 2007; 58:1–7
10. Liu X, Bi X, Huang J, Jerecic R, Carr J, Li D. Contrast-enhanced whole-heart coronary magnetic resonance angiography at 3.0 T: comparison with steady-state free precession technique at 1.5 T. *Invest Radiol* 2008; 43:663–668
11. Weiger M, Boesiger P, Hilfiker PR, Weishaupt D, Pruessmann KP. Sensitivity encoding as a means of enhancing the SNR efficiency in steady-state MRI. *Magn Reson Med* 2005; 53:177–185
12. Yu J, Schar M, Vonken EJ, Kelle S, Stuber M. Improved SNR efficiency in gradient echo coronary MRA with high temporal resolution using parallel imaging. *Magn Reson Med* 2009; 62:1211–1220
13. Ohliger MA, Grant AK, Sodickson DK. Ultimate intrinsic signal-to-noise ratio for parallel MRI: electromagnetic field considerations. *Magn Reson Med* 2003; 50:1018–1030
14. Nehrke K, Bornert P, Mazurkewitz P, Winkelmann R, Grasslin I. Free-breathing whole-heart coronary MR angiography on a clinical scanner in four minutes. *J Magn Reson Imaging* 2006; 23: 752–756
15. Okada T, Kanao S, Ninomiya A, et al. Whole-heart coronary magnetic resonance angiography with parallel imaging: comparison of acceleration in one-dimension vs. two-dimensions. *Eur J Radiol* 2009; 71:486–491
16. Sodickson DK, Manning WJ. Simultaneous acquisition of spatial harmonics (SMASH): fast imaging with radiofrequency coil arrays. *Magn Reson Med* 1997; 38:591–603
17. Griswold MA, Jakob PM, Heidemann RM, et al. Generalized autocalibrating partially parallel acquisitions (GRAPPA). *Magn Reson Med* 2002; 47:1202–1210
18. Nezafat R, Stuber M, Ouwerkerk R, Gharib AM, Desai MY, Pettigrew RI. B1-insensitive T2 preparation for improved coronary magnetic resonance angiography at 3 T. *Magn Reson Med* 2006; 55: 858–864
19. Noeske R, Seifert F, Rhein KH, Rinneberg H. Human cardiac imaging at 3 T using phased array coils. *Magn Reson Med* 2000; 44:978–982
20. Zhao JM, Clingman CS, Narvainen MJ, Kauppinen RA, van Zijl PC. Oxygenation and hematocrit dependence of transverse relaxation rates of blood at 3T. *Magn Reson Med* 2007; 58:592–597
21. Hu P, Chan J, Smink J, et al. Contrast-enhanced whole heart coronary MRI with bolus infusion of gadobenate dimeglumine at 1.5T. In: Proceedings of the 18th Joint Annual ISMRM-ESMRMB

Meeting. Berkeley, CA: ISMRM, 2010:1236
22. Nassenstein K, Breuckmann F, Hunold P, Barkhausen J, Schlosser T. Magnetic resonance coronary angiography: comparison between a Gd-BOPTA– and a Gd-DTPA–enhanced spoiled gradient-echo sequence and a non-contrast-enhanced steady-state free-precession sequence. *Acta Radiol* 2009; 50:406–411
23. Pintaske J, Martirosian P, Graf H, et al. Relaxivity of gadopentetate dimeglumine (Magnevist), gadobutrol (Gadovist), and gadobenate dimeglumine (MultiHance) in human blood plasma at 0.2, 1.5, and 3 Tesla. *Invest Radiol* 2006; 41:213–221
24. Jahnke C, Nehrke K, Paetsch I, et al. Improved bulk myocardial motion suppression for navigator-gated coronary magnetic resonance imaging. *J Magn Reson Imaging* 2007; 26:780–786
25. National Electrical Manufacturers Association. Determination of signal-to-noise ratio (SNR) in diagnostic magnetic resonance imaging. Publication NEMA MS 1-2008: Rosslyn, VA: National Electrical Manufacturers Association, 2008
26. Botnar RM, Stuber M, Danias PG, Kissinger KV, Manning WJ. Improved coronary artery definition with T2-weighted, free-breathing, three-dimensional coronary MRA. *Circulation* 1999; 99: 3139–3148
27. Etienne A, Botnar RM, Van Muiswinkel AM, Boesiger P, Manning WJ, Stuber M. "Soap-bubble" visualization and quantitative analysis of 3D coronary magnetic resonance angiograms. *Magn Reson Med* 2002; 48:658–666
28. Austen WG, Edwards JE, Frye RL, et al. A reporting system on patients evaluated for coronary artery disease: report of the Ad Hoc Committee for Grading of Coronary Artery Disease, Council on Cardiovascular Surgery, American Heart Association. *Circulation* 1975; 51(suppl):5–40
29. Huber ME, Paetsch I, Schnackenburg B, et al. Performance of a new gadolinium-based intravascular contrast agent in free-breathing inversion-recovery 3D coronary MRA. *Magn Reson Med* 2003; 49:115–121
30. Saeed M. New concepts in characterization of ischemically injured myocardium by MRI. *Exp Biol Med (Maywood)* 2001; 226:367–376
31. Maintz D, Ozgun M, Hoffmeier A, et al. Selective coronary artery plaque visualization and differentiation by contrast-enhanced inversion prepared MRI. *Eur Heart J* 2006; 27:1732–1736
32. Bluemke DA, Achenbach S, Budoff M, et al. Noninvasive coronary artery imaging: magnetic resonance angiography and multidetector computed tomography angiography: a scientific statement from the American Heart Association Committee on Cardiovascular Imaging and Intervention of the Council on Cardiovascular Radiology and Intervention, and the Councils on Clinical Cardiology and Cardiovascular Disease in the Young. *Circulation* 2008; 118:586–606
33. Fischer RW, Botnar RM, Nehrke K, Boesiger P, Manning WJ, Peters DC. Analysis of residual coronary artery motion for breath hold and navigator approaches using real-time coronary MRI. *Magn Reson Med* 2006; 55:612–618
34. Kotys MS, Herzka DA, Vonken EJ, et al. Profile order and time-dependent artifacts in contrast-enhanced coronary MR angiography at 3T: origin and prevention. *Magn Reson Med* 2009; 62:292–299
35. Bhat H, Lai P, Li D. Self-tracking of contrast kinetics for automatic triggering of contrast-enhanced whole-heart coronary magnetic resonance angiography. *J Magn Reson Imaging* 2009; 29: 809–816